ELSEVIER

Journal of Power Sources 81–82 (1999) 554–557

JOURNAL OF POWER SOURCES

www.elsevier.com/locate/jpowsour

Electrochemical STM observation of $LiMn_2O_4$ thin films prepared by pulsed laser deposition

Minoru Inaba *, Takayuki Doi, Yasutoshi Iriyama, Takeshi Abe, Zempachi Ogumi

Department of Energy and Hydrocarbon Chemistry, Graduate School of Engineering, Kyoto University, Sakyo-ku, Kyoto 606-8501, Japan

Abstract

Spinel $LiMn_2O_4$ thin films were prepared by pulsed laser deposition. The surface morphology change of the film with potential cycling between 3.5 and 4.25 V was observed in 1 M $LiClO_4$/PC by electrochemical scanning tunneling microscopy. After cycling, small round-shaped particles of 120–250 nm in diameter appeared on the surface. The number of the newly formed particles increased with repeated cycling while the size decreased. The observed morphology change suggested that the small particle were formed from the solution through a kind of dissolution/precipitation reactions. © 1999 Elsevier Science S.A. All rights reserved.

Keywords: Lithium-ion battery; Lithium manganese oxide; STM; Capacity fading

1. Introduction

Spinel $LiMn_2O_4$ is a promising material for use as 4-V positive electrode in rechargeable lithium batteries because of its economical and environmental advantages [1–3]. However, spinel $LiMn_2O_4$ has a drawback to be improved; that is, the capacity fades rapidly upon charge/discharge cycling. Several possible mechanisms for the capacity fading of spinel $LiMn_2O_4$ have been proposed: (i) electrolyte decomposition at high potentials [4], (ii) slow dissolution of $LiMn_2O_4$ through the disproportionation reaction: $2Mn^{3+} \rightarrow Mn^{4+} + Mn^{2+}$ [4], (iii) an irreversible structural transition due to Jahn–Teller distortion at the discharged state [4,5], and (iv) a transformation of the unstable two-phase structure in the higher potential region to a more stable single-phase structure via loss of MnO [6]. Although all these factors more or less seem to participate in the capacity fading of $LiMn_2O_4$, the primary reason has not been identified yet.

Electrochemical scanning tunneling microscopy (STM) is a useful tool to observe morphology changes. In situ observation by STM enables us to obtain direct information about what is taking place on an electrode surface in solution, which is the greatest advantage over other tools for microscopic observation such as scanning electron microscopy because electrodes in rechargeable lithium batteries are usually vulnerable to air and moisture. We have so far applied this technique to clarify the mechanism of passive film formation on graphite negative electrode in rechargeable lithium batteries [7–10]. In the present study, this technique is applied to spinel $LiMn_2O_4$ positive electrode. If a surface reaction is involved in the capacity fading, STM observation of the surface morphology change will give important insight about the mechanism of the capacity fading. In STM observation, the surface of a sample should be as flat as possible to obtain images of good resolution. We therefore prepared $LiMn_2O_4$ thin films by pulsed laser deposition (PLD) as sample electrodes and observed the morphological change of the film surface by electrochemical STM to elucidate the mechanism for the capacity fading.

2. Experimental

A sintered Li–Mn–O pellet was used as a target of PLD. A mixture of $LiNO_3$ (Wako, 99.9% purity) and MnO_2 (Wako, 99.5% purity) in a lithium-excess ratio of $Li/Mn = 0.7$ was fired at 450°C for 24 h in O_2. The powder was ground, pressed into pellets, and sintered at 750°C for 48 h.

PLD was conducted in a vacuum chamber made of stainless steel. A KrF excimer laser (Japan Storage Batteries, Model EXL-210) was used a light source. The target was irradiated with the laser beam through a SiO_2 glass

* Corresponding author. Tel.: +81-75-753-4933; Fax: +81-75-753-5889; E-mail: inaba@scl.kyoto-u.ac.jp

0378-7753/99/$ - see front matter
PII: S0378-7753(99)00215-3

window. The energy fluence of the beam was fixed at 2 J cm^{-2} with a repetition frequency of 10 Hz. The base pressure of the vacuum chamber was $< 1 \times 10^{-4}$ Pa. Oxygen gas was introduced into the chamber and the pressure was maintained at 27 Pa. Thin films of $LiMn_2O_4$ were deposited on Pt or Au substrates heated at 873 K for 1–3 h. After deposition, the substrate was cooled slowly at 1 K min^{-1}. X-ray diffraction (XRD) patterns of the thin films were obtained with a Shimadzu XD-D1 diffractometer equipped with a Cu K_α source. The total mass and the Li/Mn ratio of deposited thin films were analyzed by inductively coupled plasma (ICP) spectroscopy (Shimadzu, ICP-1000II).

For electrochemical and STM measurements, thin films deposited on Au substrates for 1 h were used. The thickness of the films was about 0.3 μm. Electrochemical properties of the thin films were measured using a three-electrode cell. The effective electrode surface area was limited at 0.19 cm^2 by an O-ring. The solution was 1 M $LiClO_4$ dissolved in propylene carbonate (PC) (Mitsubishi Chemicals, Battery Grade). Both reference and counter electrodes were lithium metal. Charge and discharge tests and cyclic voltammetry experiments were carried out at a constant current of 5.3 μA cm^{-2} and at a scan rate of 1 mV s^{-1}, respectively, between 3.5 and 4.25 V.

STM observation coupled with cyclic voltammetry was carried out with an SPI-3600 system (SEIKO Instruments). The configuration of the electrochemical STM cell was described elsewhere [8]. A $LiMn_2O_4$ thin film was mounted at the bottom of the cell. The electrolyte solution was 1 M $LiClO_4$ dissolved in propylene carbonate (PC). The counter and reference electrodes were platinum wire and lithium metal, respectively. An apiezone wax-coated Pt/Ir tip was used for STM observation. Before cyclic voltammetry, STM images of the film surface were obtained at sample and tip potentials of 3.5 and 3.0 V, respectively, at a tip scan rate of 1 μm s^{-1}. Cyclic voltammetry was carried out at a sweep rate of 1 mV s^{-1} between 3.5 and 4.25 V. During cyclic voltammetry measurements, the tip was lifted outside of the tunneling region to avoid an accidental contact with the sample. After the potential cycling, STM images were obtained at a sample potential of 3.5 V to observe the morphology change that occurred during the potential cycling. This procedure was repeated up to 75 potential cycles.

All measurements were carried out at room temperature in an argon-filled glove box. The dew point in the glove box was kept below −60°C. The water content in the solution was less than 30 ppm.

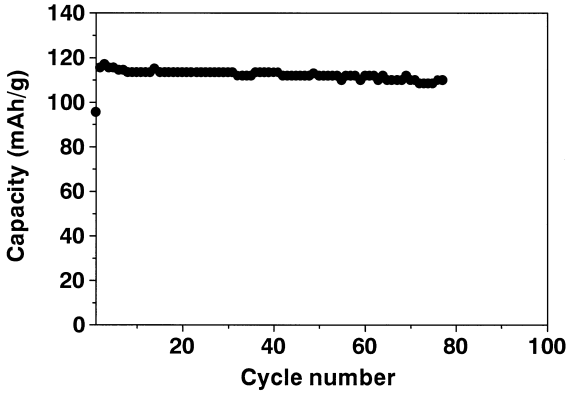

Fig. 2. Variation of the discharge capacity with cycle number for $LiMn_2O_4$ thin film deposited on Au at 873 K for 1 h. The charge/discharge test was conducted at a constant current of 5.3 μA cm^{-2} in 1 M $LiClO_4$/PC.

3. Results and discussion

3.1. Characterization of $LiMn_2O_4$ thin film

Fig. 1 shows the XRD pattern of a film deposited on Pt at 873 K for 3 h. The pattern indicates that single-phase spinel $LiMn_2O_4$ was obtained by PLD. The peaks at 2θ angles of 18.6°, 36.1°, 37.9°, and 44.1° correspond to the (111), (311), (222), and (400) diffraction lines, respectively [11]. The peaks at 39.8°, 46.2°, and 67.5° are assigned to diffraction lines of Pt, and the peak at 22.6° to a line of an adhesive tape used to fix the film on the sample folder. ICP measurements revealed that the Li/Mn atomic

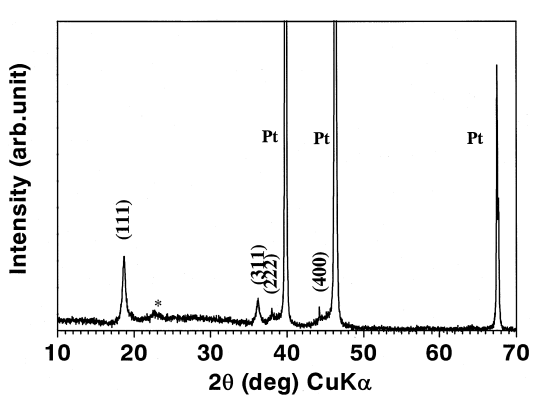

Fig. 1. XRD pattern of $LiMn_2O_4$ thin films prepared on Pt at 873 K for 3 h. *Adhesive tape.

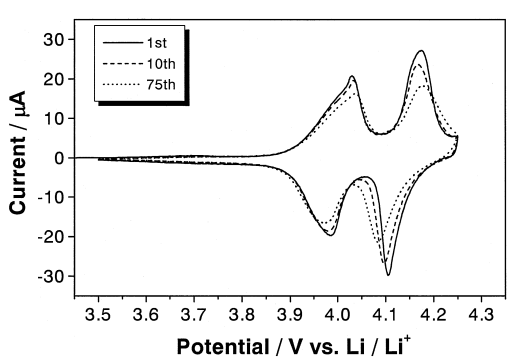

Fig. 3. Cyclic voltammograms of $LiMn_2O_4$ thin film deposited on Au at 873 K for 1 h. The electrolyte solution was 1 M $LiClO_4$/PC. The scan rate was 1 mV s^{-1}.

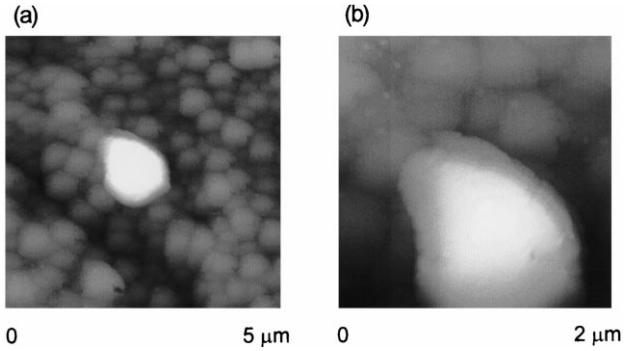

Fig. 4. STM images of $LiMn_2O_4$ thin film obtained in 1 M $LiClO_4$/PC before cycling. The sample and tip potentials were 3.5 and 3.0 V, respectively. (a) 5×5 μm, (b) 2×2 μm.

ratio of the film was 0.51; that is, x in $Li_xMn_2O_4$ was 1.02. The deposition rate estimated from the total mass of the film was 6.2×10^{-5} g cm^{-2} h^{-1} (3.4×10^{-7} mol cm^{-2} h^{-1}).

3.2. Electrochemical properties of $LiMn_2O_4$ thin film

Charge and discharge tests were conducted at a constant current of 5.3 μA cm^{-2} for a $LiMn_2O_4$ thin film deposited on Au at 873 K for 1 h. Fig. 2 shows the variation of the discharge capacity. The initial discharge capacity was around 115 mA h g^{-1} except in the first cycle (96 mA h g^{-1}). The capacity gradually decreased with cycle number and faded by about 6% of the initial capacity in the 75th cycle.

Fig. 3 shows cyclic voltammograms of a thin film deposited under the same conditions as above. Cyclic voltammetry showed two couples of redox peaks at around 4.0 and 4.1 V, which are characteristic of $LiMn_2O_4$ [12]. The peaks, in particular, the couple at ca. 4.1 V were broadened and the peak separation became larger after repeated cycling. The observed peak broadening and increase in peak separation suggest that some changes in the composition and/or in the grain size of the film took place during potential cycling. The discharge capacity in each cycle was estimated from the area of the reduction peaks. In the 75th cycle, the capacity was smaller by 7% than that in the first cycle, which was in agreement with the result obtained from the charge and discharge test in Fig. 3. Consequently, it is inferred that the observed peak broadening and increase in peak separation are responsible for the capacity fading.

3.3. STM observation of $LiMn_2O_4$ thin film before and after cyclic voltammetry

STM images of as-prepared thin film obtained at 3.5 V in $LiClO_4$/PC are shown in Fig. 4. The film consisted mostly of small grains of about 400 nm in diameter. At the center of Fig. 4a, a large particle of 1-μm diameter was observed. We used it as a guide to find the identical region in further observation. Fig. 5 shows the morphology change of the surface after potential cycling between 3.5 and 4.25 V. After one cycle (Fig. 5a), small fragments of ca. 100 nm in diameter appeared on the surface. The large particle was seen in the lower part of the image, which confirms that the image shows nearly the same region as Fig. 4b. The original $LiMn_2O_4$ grains of 400-nm diameter were still observed below the small particles. Remarkable changes were not observed up to 10 cycles except that the number of the fragments decreased gradually with cycling. The surface morphology suddenly changed after 20 cycles (Fig. 5b); that is, many small particles appeared on the surface. The size of the newly formed particles was in the range of 120–250 nm. After 75 cycles (Fig. 5c), the particle size decreased further to about 70 nm while the number of the particles increased.

As mentioned earlier, it is widely known that manganese ions dissolve in the solution during charging and discharging [13,14], which has been claimed as one of the reasons for the capacity fading. However, such dissolution of manganese ions does not explain the morphology changes in Fig. 5. It should be noted that the newly formed small particles after 20 cycles did not have sharp edges, but had a relatively round shape, which clearly shows that the particles were not formed by the fracture of the original grains. In addition, part of the large 1-μm particle,

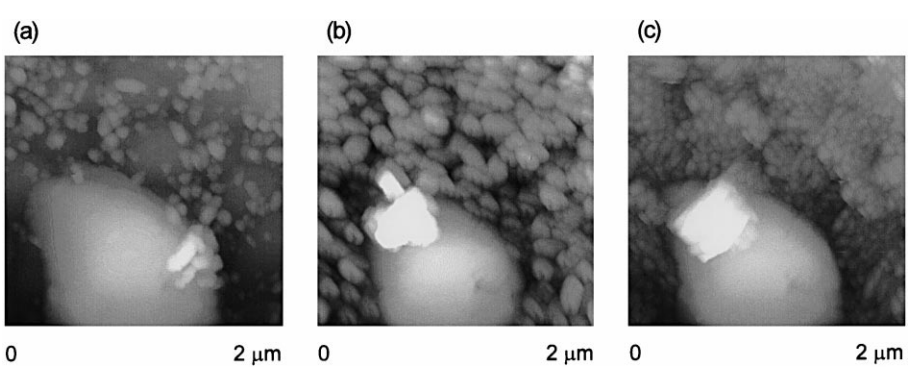

Fig. 5. STM images (2 × 2 μm) of $LiMn_2O_4$ thin film obtained after (a) 1, (b) 20, and (c) 75 cycles between 3.50 V and 4.25 V in 1 M $LiClO_4$/PC. The sample and tip potentials were 3.5 and 3.0 V, respectively.

which was used as a guide, was buried by the layer of the newly formed small particles after repeated cycling in Fig. 5b and c. These facts suggest that the small particles were formed from the solution and deposited on the original surface. Although the composition of the particles are not known, it is most likely that the particles were Li–Mn–O and were formed through some kind of dissolution/precipitation reactions. The newly formed particles may be of less crystallinity or have a composition different from the original $LiMn_2O_4$, which would cause the capacity fading of spinel $LiMn_2O_4$ positive electrode. During dissolution/precipitation reactions, part of dissolved manganese ions in the vicinity of the surface diffuse away into the bulk of the solution, which would result in the so-called dissolution of manganese ions reported so far in the literature. Further STM observation is now in progress to clarify the correlation between the capacity fading and small particle formation in detail.

4. Conclusions

Spinel $LiMn_2O_4$ thin films were prepared by PLD as sample electrodes. The discharge capacity decreased by 6% of the initial capacity after 75 charge/discharge cycles in the range 3.5 to 4.25 V in 1 M $LiClO_4$/PC. Cyclic voltammetry experiments revealed that redox peaks broadened after repeated cycling. The surface morphology change of the thin film after potential cycling was observed in the solution by electrochemical STM. Before cycling, the film consisted of $LiMn_2O_4$ grains of ca. 400-nm diameter. After repeated cycling, smaller particles appeared and covered the surface. The number of the newly formed particles increased with repeated cycling while the size decreased. The observed morphology change suggested that the newly formed small particles were formed from the solution through a kind of dissolution/precipitation reactions.

Acknowledgements

This work was partly supported by a Grant-in-Aid for Scientific Research (No. 10750593) from the Ministry of Education, Science, Sports and Culture, Japan.

References

[1] T. Ohzuku, M. Kitagawa, T. Hirai, J. Electrochem. Soc. 137 (1990) 769.
[2] J.M. Trascon, E. Wang, F.K. Sholoohi, W.R. McKinnon, S. Colson, J. Electrochem. Soc. 138 (1991) 2859.
[3] Y. Xia, M. Yohsio, J. Power Sources 56 (1995) 61.
[4] R.J. Gummow, A. de Kock, M.M. Thackeray, Solid State Ionics 69 (1994) 59.
[5] M.M. Thackeray, Y.S. Horn, A.J. Kahaian, K.D. Kepler, E. Skinner, J.T. Vaughey, S.A. Hackney, Electrochem. Solid-State Lett. 1 (1998) 7.
[6] Y. Xia, Y. Zhou, M. Yoshio, J. Electrochem. Soc. 144 (1997) 2593.
[7] M. Inaba, Z. Siroma, A. Funabiki, Z. Ogumi, T. Abe, Y. Mizutani, M. Asano, Chem. Lett., 1995, pp. 661.
[8] M. Inaba, Z. Siroma, A. Funabiki, Z. Ogumi, T. Abe, Y. Mizutani, M. Asano, Langmuir 12 (1996) 1535.
[9] M. Inaba, Z. Siroma, Y. Kawatate, A. Funabiki, Z. Ogumi, J. Power Sources 68 (1997) 221.
[10] M. Inaba, Y. Kawatate, A. Funabiki, T. Abe, Z. Ogumi, Electrochim. Acta, submitted.
[11] JCPDS No. 35-0782.
[12] I. Uchida, H. Fujiyoshi, S. Waki, J. Power Sources 68 (1997) 139.
[13] D.H. Jang, T.J. Shin, S.M. Oh, J. Electrochem. Soc. 143 (1996) 2204.
[14] A. Blyr, C. Sigala, G. Amatucci, D. Guyomard, Y. Chabre, J.-M. Trascon, J. Electrochem. Soc. 145 (1998) 194.